Scientific Research Publishing

Open Journal of Biophysics, 2018, 8, 163-175
http://www.scirp.org/journal/ojbiphy
ISSN Online: 2164-5396
ISSN Print: 2164-5388

Specific Radius Change of Quantum Dot inside the Lipid Bilayer by Charge Effect of Lipid Head-Group

Soon Ki Sung[1,2*], Hyuk Kyu Pak[3*], Jong Hyeok Kwak[4], Sang Weon Lee[1], Young Ha Kim[1], Beong Ik Hur[5], Seong Jin Jin[6], Gyeong Rip Kim[1,2#†]

[1]Department of Neurosurgery, Pusan National University Yang-san Hospital, Yang-san, Korea
[2]Research Institute for Convergence of Biomedical Science and Technology, Yang-san, Korea
[3]Department of Physics, Ulsan National Institute of Science and Technology, Ulsan, Korea
[4]Department of Radiology, Pusan National University Yang-san Hospital, Yang-san, Korea
[5]Department of Neurosurgery, Pusan National University Hospital, Busan, Korea
[6]Haeundae Paik Hospital, Busan, Korea
Email: [†]sjkim76@pusan.ac.kr

How to cite this paper: Sung, S.K., Pak, H.K., Kwak, J.H., Lee, S.W., Kim, Y.H., Hur, B.I., Jin, S.J. and Kim, G.R. (2018) Specific Radius Change of Quantum Dot inside the Lipid Bilayer by Charge Effect of Lipid Head-Group. *Open Journal of Biophysics*, **8**, 163-175.
https://doi.org/10.4236/ojbiphy.2018.83012

Received: June 12, 2018
Accepted: July 22, 2018
Published: July 25, 2018

Abstract

We studied the quantum dot-liposome complex (QLC), which is the giant unilamellar vesicle with quantum dots (QDs) incorporated in its lipid bilayer. A spin coating method in conjunction with the electroformation technique yielded vesicles with highly homogeneous unilamellar structure. We observed QD size dependence of the QLC formation: QLCs form with blue, green and yellow-emission QD (core radius ~1.05 nm, 1.25 nm and 1.65 nm) but not with red-emission QD (core radius ~2.5 nm). In order to explain this size dependence, we made a simple model explaining the QD size effect on QLC formation in terms of the molecular packing parameter and the lipid conformational change. This model predicts that QDs below a certain critical size (radius ≈ 1.8 nm) can stably reside in a lipid bilayer of 4 - 5 nm in thickness for Egg-PC lipids. This is consistent with our previous experimental results. In the case of red-emission QD, QD-aggregations are only observed on the fluorescent microscopy instead of QLC. We expected that the reduction of packing parameter (P) would lead to the change of specific QD radius. This prediction could be verified by our experimental observation of the shift of the specific QD size by mixing DOPG.

Keywords

Quantum Dot-Liposome Complexes (QLCs), The Interface Energy at Optical Head Area, Packing Parameter, DOPC/DOPG QLC

*Contributed equally to this work.
#Corresponding author earlier know as Seong Jin Kim.

1. Introduction

Labeling biomolecules and cells with organic fluorophores are representative tools for studying the underlying complex interactions and the dynamics in metabolic processes in various time and length scales. Recently, these organic fluorophores have been gradually replaced by nano-size semiconductor nanocrystals [1] such as quantum dots (QDs).

This preference for QDs results from several remarkable optical properties of QDs. In contrast to organic fluorophores, QDs have a higher quantum yield, and a narrower and more symmetric emission spectrum which can be controlled by tuning the core size of the QDs during synthesis procedures. Furthermore, the photo-bleaching effect of QDs is much weaker compared to organic fluorophores. However, before introduction into biological environments, the surface of QDs should be transformed to hydrophilic with the help of amphiphilic molecules or other surface-capping materials due to the hydrophobic surface property of QDs. In recent years, several groups reported passivation of QDs by phospholipid, which is a building unit of the cell membrane [2]-[11]. One good example is QLC (Quantum dot-Liposome Complex) which is a giant unilamellar vesicle with QDs incorporated in the lipid bilayer [12] [13] [14] [15].

QLC is good candidate for biomedical imaging in site of specific drug delivery. For instance, biological fusion area between QLCs and biological targets can be fluorescent by conjugating with QDs and macromolecules such as cell membrane [12]. In addition, if QDs coexist with organic fluorophores in the lipid bilayer of QLCs, fluorescence resonance energy transfer (FRET) signal can be observed in a nano-scale confined system of a lipid bilayer [16].

In spite of the various potential applications of QLCs, we still lack detailed knowledge and quantitative approaches regarding the interactions and dynamics between QDs and lipids during QLC formation. And there is still no reliable experimental data regarding the exact position of QDs in the lipid bilayer. In this work, we assume that QDs are approximated as hydrophobic hard spherical particles, and there are no specific interactions other than hydrophobic interactions. Therefore, QDs are spontaneously incorporated into the lipid bilayer of lipsomes during the self-assembly process due to strong hydrophobic interactions between QDs and phospholipids in hydrophilic environment and are positional at the center of the lipid bilayer.

In our previous work, we proposed a theoretical model by interfacial energy for a quantum dot (QD)-lipid mixed system based on a simple geometrical assumption for a single-component lipid (DOPC) monolayer deformation profile [13] [14]. And we studied the stability problem of QDs inside the lipid bilayer depending on the size of QD as shown **Figure 1** and experimentally proposed QLCs, which are GUVs (Giant Unilamellar Vesicles) with QDs below critical QD size loaded into the DOPC lipid bilayer. But, in our previous study, we did not observe any QLCs for the orange-emission QDs (2 - 2.15 nm) and red-emission ones (~2.5 nm) above specific QD size [15].

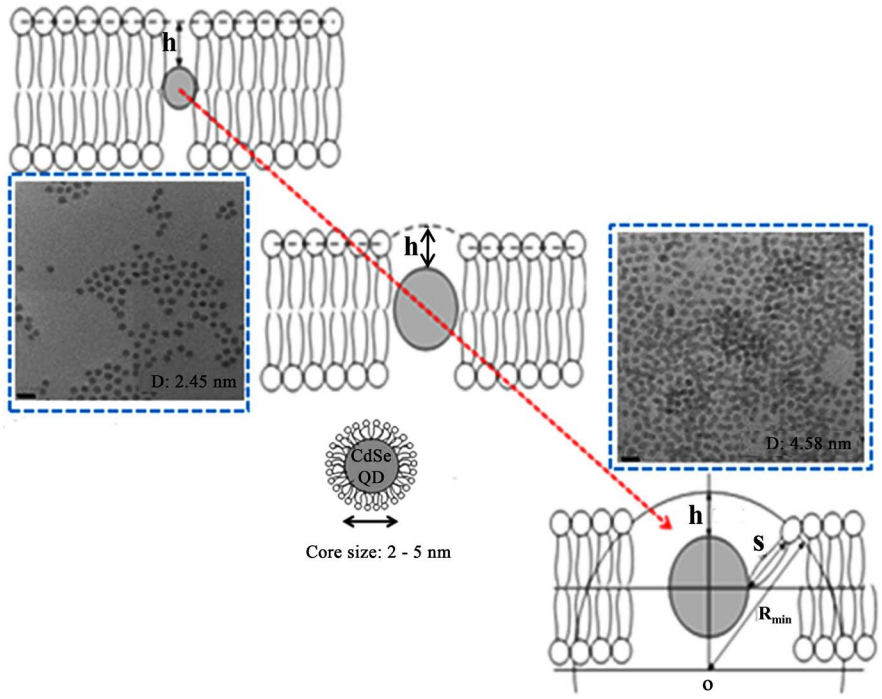

Figure 1. QD is embedded in the thin lipid bilayer depending on the size of QD. Box dotted line shows TEM image of CdSe-QD: left QD size D: 2.45 nm and right QD size D: 4.58 nm. This scale bar is about 10 (nm).

In the present work, however, we do detect a fluorescent signals from orange-emission QDs (~2 - 2.15 nm) and red-emission QDs (~2.5 nm) above critical QD size in the mixture of DOPC and DOPG. To interpret these experimental results, we propose a simple theoretical model based on geometric considerations of deformed lipid monolayer surrounding a QD in terms of the molecular packing parameter and the conformational change of the lipid chain instead of complicated elastic free energy calculations. This model explains our experimental observation of shift of the specific QD size.

2. Background and Model

According to Israelachvili's work [17], given the packing parameter P of a given lipid, the minimum radius $R_{\min}$ of the special liposome is determined as follow. **Figure 2** shows a uni-bilayer liposome with the in-outer layer (R_0) and the outer layer thickness (t_0) in a single liposome. For liposome of the outer layer volume V_0 and the outer surface area S_0 with N_0 molecules, there are following relations between them [18].

$$V_0 = N_0 v = \frac{4}{3}\pi\left[R_0^3 - \left(R_0 - t_0\right)^3\right] \tag{1}$$

$$S_0 = 4\pi R_0^2 = N_0 a, \quad N_0 = \frac{4}{3v}\pi\left[R_0^3 - \left(R_0 - t_0\right)^3\right] \tag{2}$$

Here, v is the volume of simple hydrocarbon molecule. The area per head group (a) is

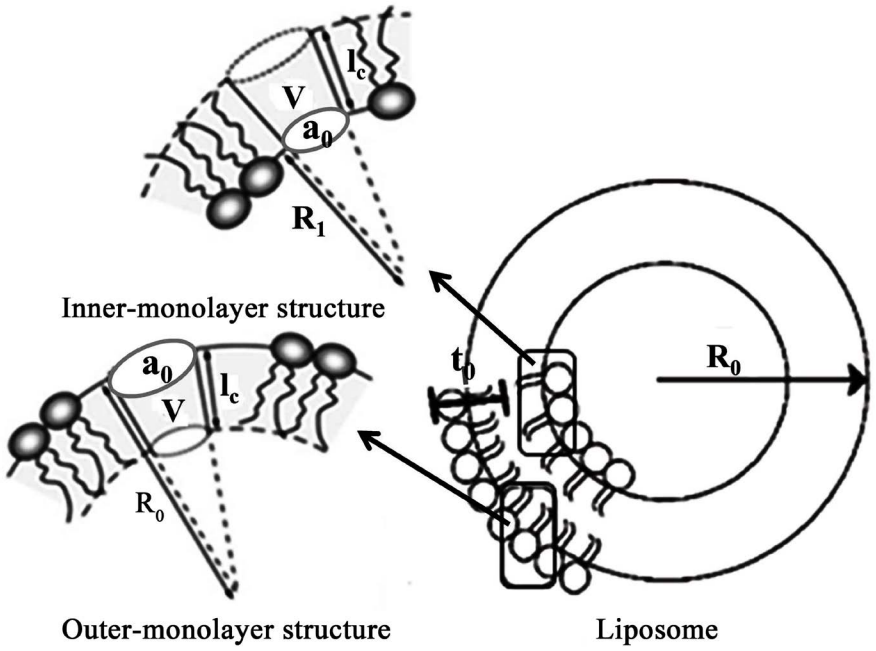

Figure 2. Uni-bilayer liposome and inner and outer monolayer structures.

$$a = 4\pi R_0^2 / N_0 = 3vR_0^2 \Big/ \left[R_0^3 - \left(R_0 - t_0 \right)^3 \right] \tag{3}$$

Here, ($a \neq a_0$) is the actual area per head group. If Equation (3) is divided by a_0, the ratio of the actual area a to the optimal area a_0 is given by

$$\frac{a}{a_0} = 3\left(\frac{v}{a_0 l_c} \right) l_c \frac{R_0^2}{\left[R_0^3 - \left(R_0 - t_0 \right)^3 \right]} \tag{4}$$

Here, a_0 is referred to as the optimal surface area per molecule, defined at the hydrocarbon-water interface.

Equation (4) gives the area ratio as a function of the packing parameter ($P = v/a_0 l_c$), the critical chain length (l_c), the out radius (R_0), and the thickness of the outer layer (t_0). If the packing parameter and critical chain length are fixed, the ratio of the area to the optima head area (a/a_0) will approaches 1 with a decrease of the out radius (R_0). This condition approaches to the lower possibility for liposome formation. When the minimum value of R_0 is reached, the smallest liposome can be formed. The out radius (R_0) replace the value of $R_{\min}$, we refers to $t_0 = l_c$. Substituting $a/a_0 = 1$, and $t_0 = l_c$, expressed as a formula according to $R_{\min}$,

$$\left(1 - \frac{v}{a_0 l_c} \right) R_{\min}^2 - l_c R_{\min} + \frac{l_c^2}{3} = 0 \tag{5}$$

From Equation (5), the minimum radius is

$$R_{\min} = \frac{3 + \sqrt{3(P-1)}}{6(1-P)/l_c} \tag{6}$$

Here, the packing parameter is $P = v/a_0 l_c$.

For truly fluid hydrocarbon chains, meanwhile, the optimal head area should not depend strongly on the chain length or on the number of chains. We can define the critical chain l_c as the maximum effective length of the hydrocarbon chain in the liquid state. The semi-empirical definition of the hydrocarbon chain length was theoretically interpreted by Israelachvili [17] Tanford [19] and Lindman [20]. l_c for the saturated hydrocarbon chains is

$$l_c \le l_{\max} = (0.154 + 0.1265n)\ \text{nm} \tag{7}$$

Here, $l_{\max}$ stands for the length of the fully extended hydrocarbon chain, and n is number of carbon atom for each hydrocarbon tail. However, as may be expected, l_c is of the same order as, though somewhat less than, the fully extended molecular length of the chain $l_{\max}$. It can be seen that the minimum size of a liposome ($R_{\min}$) depends on the packing parameter ($P = v/a_0 l_c$) and on the critical chain length (l_c). Since v and l_c are fixed, the only way to reduce the packing parameter ($v/a_o l_c$) is increasing the optimal head area (a_0).

Modeling

The key point of this model would define the critical QD radius by limiting the $l_{\max}$ to cover part of the void around the QD $S_{\max}$ at graph. For the definition of $S_{\max}$ in this model, we considered only the size of QD core excluding ligand (hexadecylamine).

Equation (6) shows the minimum possible radius $R_{\min}$ of the spherical liposome, which is composed of the lipids with the packing parameter *P*. We first assumed that the maximum possible curvature of the lipid monolayer with thickness *d* around the QD of radius *r* has its limit at the value $1/R_{\min}$ to evade any unfavorable surface energy penalties. In other words, $R_{\min}$ is the critical radius below which a bilayer cannot curve without introducing unfavourable packing strains such as QD inside the lipids. Therefore, when the size of each QD is smaller than $R_{\min}$, as in our experiment, the curvature of the monolayer around the QD is approximated as $1/R_{\min}$, and the deformed monolayer profile is a circular arc of radius as $R_{\min}$ shown in **Figure 4**. In the case of Egg-PC lipid liposome, the packing parameter value is known to be 0.85 ($v/a_0 l_c$; $a_0 \approx 0.717\ \text{nm}^2$, $v \approx 1.063\ \text{nm}^3$ and $l_c \approx 1.75$ nm) [17]. Therefore, we know that $R_{\min}$ of Egg-PC liposome can get the value of 10.8 nm from Equation (6).

We can also introduce two parameters related to the conformational variation of the hydrocarbon chain around the QD: the compressing extent *h* of the hydrocarbon chain and the maximum stretching extent *S* of the hydrocarbon chain in order to remove void formation around the QD. In the case of Egg-PC lipid, a saturated hydrocarbon chain is approximately composed of n = 18 of carbon number about 70%. When the number of carbon is n = 18, we defined $l_{\max} = 2.43$ nm form Equation (7). If S has only to contact with ligand, as shown in **Figure 3(a)**, we can also assume that the most stretched (longest) chain is

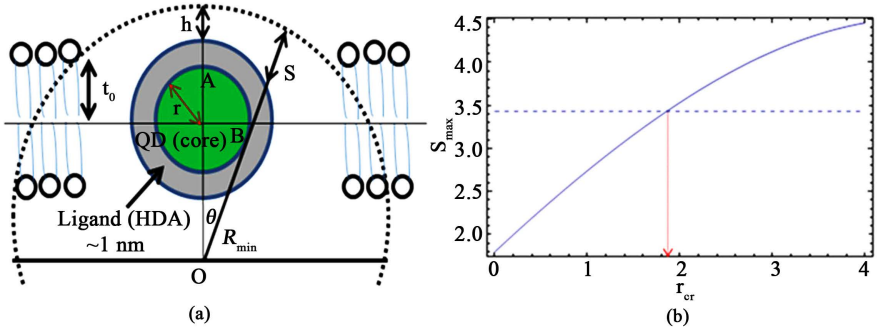

Figure 3. (a) A model representing the deformed monolayer due to the incorporation of a QD inside the lipid bilayer (b) A plot of chain length of the most stretched lipid, $S_{\max}$ as a function of the QD radius, r; The dotted line corresponds to the minimum radius $R_{\min}$ of deformed lipid monolayer around QD.

located in a corner of the QD direction (point B in **Figure 3(a)**) to remove the void formation between lipid and QD. Here, we approximately considered the distance between point B and C as ligand length (~1 nm). For the maximum extent, we can define $S_{\max}$ as 3.43 nm (the ligand length plus $l_{\max}$). And we assumed that the compression of the chain occurs at the top of the QD, as shown in **Figure 3(a)**. In the case of maximum compression, the lipid monolayer thickness at point A is represented by $h_{\min} = 1.22$ nm from the Egg-liposome thickness due to $l_{\max} = 2.43$ nm [21].

The distance S from the corner of the QD to the point on the circular arc of radius $R_{\min}$ for a given θ can be expressed as

$$S = \sqrt{\left(R_{\min}\sin\theta - r\right)^2 + \left(R_{\min}\cos\theta - R_{\min} + h_{\min} + r + 1\right)^2} \tag{8}$$

Equation (8) is differentiated with respect to θ to obtain the minimum $S_{\max}$ that is required to be equal to the chain length of the most stretched lipid among the lipids around the QD of radius r. **Figure 3(b)** shows a plot of $S_{\max}$ as a function of the QD radius r. $S_{\max}$ can't exceed the maximally stretched chain length, ligand length (~1 nm) plus $l_{\max}$, which is 3.43 nm in this case [17]. Otherwise, there would be a void formation at the ligand portion that is connected with corner of the QD. Therefore, the critical QD size is $r_{cr} \approx 1.8$ nm, where the chain is maximally stretched to $S_{\max}$ (corresponding to the horizontal dashed line in **Figure 3(b)**).

In **Figure 3(a)**, at point S, the curvature is divided by positive and negative. In the case of this model, we took only positive curvature into account. The part of negative curvature does not fully need to stretch because one of the principal curvatures is close to the monolayer spontaneous curvature of the DOPC. In other words, the regions of positive curvature require the highly curved lipids to cover the rapid increase of the area above critical, while the parts of negative curvature which have non-charged head-group can be decreasing the mechanical stress generated by a packing constraint between ligands and the head-group above critical size.

3. Experimental Methods and Materials

3.1. Materials

In this experiment, we used four different kinds of lipid molecules: L-α-phosphatidylcholine (Egg-Pc), 1,2-dioleoyl-sn-glycero-3-phosphocholine (DOPC), 1,2-dioleoyl-sn-glycero-3-[phospho-rac-(1-glycerol)] (DOPG), and 1,2-dipalmitoyl-sn-glycero-3-phosphocholine (DPPC), which were purchased from Avanti Polar Lipids. In the case of DOPC and DOPG, number of carbon atom for each hydrocarbon tail is $n = 18$ and DPPC is $n = 16$.

Before sample preparation, they were dissolved into chloroform at a determined concentration. Deionized water was obtained from a Milli-Q plus 185 (Millipore, Molsheim, France) ultra-pure water system with a resistivity of ≥18 MΩ/cm. Five different sizes of hexadecylamine (~1 nm)-coated CdSe QDs dispersed in toluene were purchased from Sigma-Aldrich. Each of them has a different core radius; blue (~1.05 nm), green (~1.25 nm), yellow (~1.65 nm), orange (2.0 - 2.15 nm) and red-emission (~2.5 nm).

3.2. Preparation of QLC

QLCs were synthesized by using the mixed solutions of QDs and phospholipids via the electroformation method [22] in conjunction with spin-coating technique [23], as shown in **Figure 4**. Egg-PC (10 mg/1ml) and a mixture of DOPC lipid: DOPG lipid = 1: 1 (5 mg/1ml, molecular weight) and QD (5 mg/1ml) was prepared with the volume ratio of mixed DOPC and DOPG lipid solution:QD solution = 700 μl:25 μl. This well-mixed solution was deposited onto the ITO substrate, then spin-coated at 600 rpm for 100 s under a stream of nitrogen gas. This QD/lipid thin film was immediately dried out in a vacuum oven for 2 h to remove excess organic solvents. A home-made chamber for electroformation was built by combining two transparent conducting indium tin oxide (ITO) substrates (4 × 4 cm^2, <50 Ω); one is clean and the other has a dried thin film

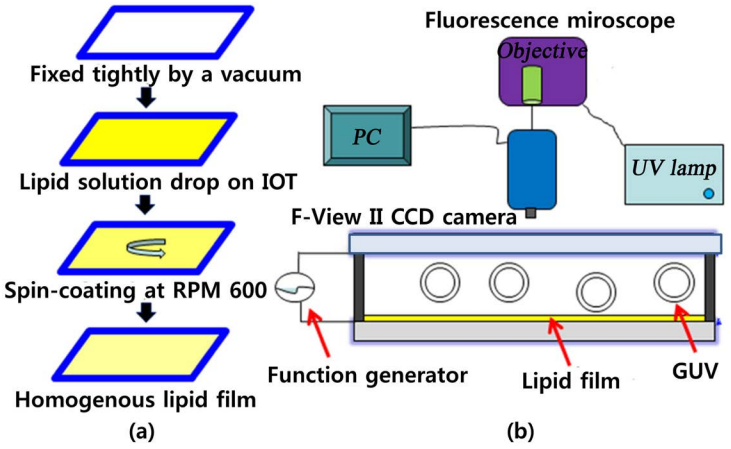

Figure 4. Preparation of QLCs in the order of spin-coating, drying-out QD/lipid thin film, and electro-swelling under an AC field. (a) Spin coating procedure (b) Schematic diagram of the electroformation setup.

with a spacer (~1 mm), then sealed with a vacuum grease (Dow Corning, High vacuum Grease). The chamber for was then filled with 2 ml of room-temperature deionized water. An AC signal of 10 Hz and 1.2 V (peak-to-peak) using a function generator (model 33250 A, Agilent, USA) was applied to the chamber for 2 h. During this process, lipiosomes grew on the substrate. Then, the AC signal was set to 4 Hz and 2.0 V (peak-to-peak) for 10min to detach the liposomes from the substrate in order to make an easy observation on a confocal microscope (Axiovert 100 M, Zeiss, German).

4. Experimental Results and Discussions

4.1. Egg-PC QLC

In order to checking this model, we checked over the QD size dependence for QD stabilization inside the lipid bilayer of liposome. The QLC is expected to be observed only for the QD size smaller than a certain specific size. We successfully obtained the blue-, green-and yellow-emission Egg-PC QLCs with clear and sharp fluorescent signals, as shown in **Figure 5(a)**. However, when red-emission QDs were used with the same concentration as the blue-, green- and yellow-emission QDs during the QLC preparation, we did not obtain the red-emission DOPC QLCs. Instead, we observed some aggregation kind of image, as shown in **Figure 5(b)**. The results are similar to those of previous DOPC experiments [15].

It means that the aggregated several QDs prefer to be surrounded by lipid instead of QLC. In other words, red-emission QDs were not incorporated into the bilayer of liposome. The experimental results are supporting the predictions of our theoretical model.

We believe that, if the QD radius is larger than r_{cr}, the QLC structure is no longer stable due to the high energy cost in the formation of either the lipid voids or increase of hydrophobic interface contacting with water, as shown in **Figure 6**. It means that the mono-layer curvature of surrounding the QD is highly required to form the QLC. In other words, we consider that hydrocarbon chain $l_{\max}$ of Egg-PC lipids is not long enough, wetting a void formation at the ligand

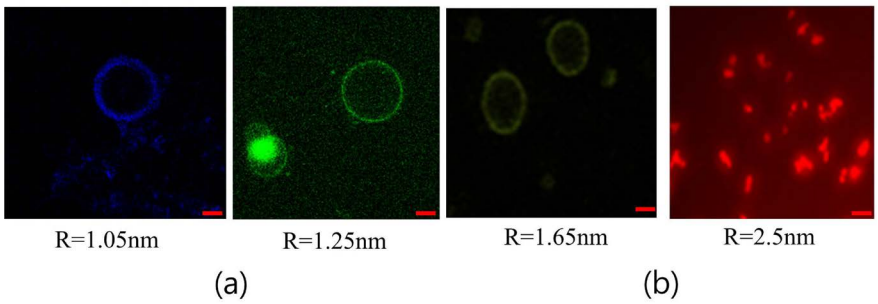

Figure 5. (a) Confocal microscope image of the blue-, green-and yellow-emission QLC with core radius ~1.05 (nm), 1.25, 1.65 (nm) (b) Aggregated QD with core radius ~2.5 (nm) surrounding lipids is observed on the fluorescent microscopy. This scale bar is about 20 (μm).

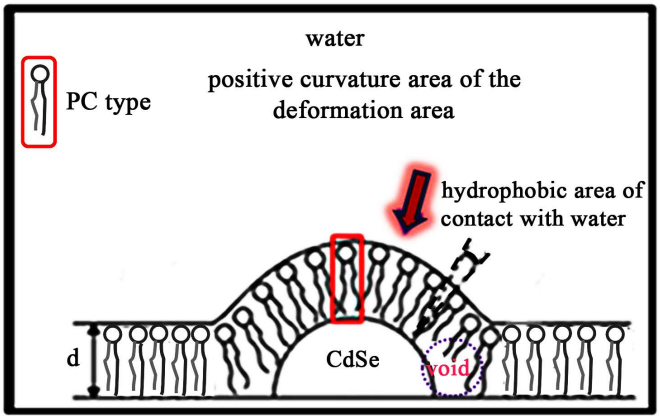

Figure 6. The mono-layer deformation of positive curvature area induced CdSe surrounding by PC-type lipid.

portion that is connected with corner of the QD and the geometric shape of them don't pack fully hydrophobic area deformed above r_{cr}. As a result, the QDs only below a certain specific size (core radius ≈ 1.8 nm) can stably reside in the lipid bilayer.

If lipids of large mono-layer curvature surrounding QD exist, they will reduce the deformation area and cover the void by highly curvature lipid. According to this model, r_{cr}, the specific radius of QD, is affected by a change in the minimum radius $R_{\min}$. In the case of Egg-PC lipid, the minimum of radius ($R_{\min}$: 10.8 nm) is given by Equation (6) and thus the maximum of radius curvature is $1/R_{\min}$. For forming the QLC above r_{cr}, it is necessary to use lipid having large monolayer curvature more than $1/R_{\min}$. It is theoretically difficult to reduce the curvature value of $1/R_{\min}$ more than 1/10.8 nm^{-1} for a single lipid molecule of the PC type.

According to the experimental result by Israelachvili [17], they have experimentally seen that it reduced the $P \approx 0.37$ (non-spherical micelle) to the $P \approx 0.33$ (spherical micelle) for sodium dodecyl sulphate surfactant (SDS) in water. Since v and l_c are fixed, the only way to reduce is to raise a_0 by raising the pH of the solution. In practice, this could be achieved by increasing the pH of the solution. This would increase the degree of ionization of the negatively charged head-groups which increases the repulsion between them, resulting in an increase in a_0. It means that the spherical micelle is more high curvature than non-spherical micelle. By Israelachvili's experiment, in this study, we think that charged lipids (DOPG) with large optimal head area (a_0) is able to from a highly mono-layer curvature more than $1/R_{\min}$ by mixing the DOPC and DOPG.

4.2. DOPC/DOPG QLC

Figure 7 shows that r_{cr} is changed by the reduction of P value. Figure 7 is not a measured value but a calculated value by Figure 3(b), which the decrease of P resulted in the decrease of $R_{\min}$ from Equation (6). The graph of Figure 3(b) shifted to the right due to the decrease of $R_{\min}$. This caused r_{cr} to shift to the

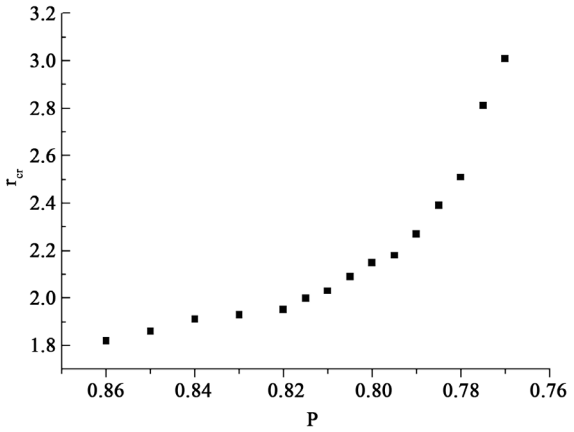

Figure 7. The change of critical point r_{cr} according to changing P.

right. In other words, the reduction of $R_{\min}$ can cause high curvature. It means that an increase in optimal head area (a_0) results in highly curvature.

We seek to increase the large optimal head area (a_0) to form a highly mono-layer curvature for checking the change of r_{cr}. In this study, if v and l_c are fixed, the only way to reduce $P = v/a_0 l_c$ is to raise optimal head area (a_0) by using the DOPG. We have the following experiment to confirm the increase of r_{cr} such as **Figure 7**.

As we mentioned earlier, QLC above r_{cr} will be formed by mixing DOPG with a charged heap-group and DOPC a neutral head-group for charge effect [17] [24].

We expected that this mixing would will be larger curvature than $1/R_{\min}$ because of the increase of effective head-group area (a_{e0}), which arises from the repulsive interaction between the like-charged head-groups. It causes the geometry shape such as **Figure 8(a)**. The phenomenon of effect head-group area explains as follows. For example, the micelle-forming lysolecithin ($v/a_0 l_c < 0.5$) and non-aggregate forming cholesterol ($v/a_0 l_c > 1.0$) will mix in certain proportions to form liposome ($0.5 < v/a_0 l_c < 1$). If we mix DOPC and DOPG, we will expect that the mono-layer of the mixture of DOPC/DOPG lipids can form more a highly curvature mono-layer than Egg-PC mono-layer.

In this experiment, we observed the orange (radius; 2.0 - 2.15 nm) and red-emission QDs (radius ~2.5 nm) were successfully incorporated in the bilayer of the mixture of DOPC/DOPG lipids, as shown in **Figure 8(b)**. This experiment result shows that the radius of curvature is increased by DOPG.

As we have anticipated the change of a specific point r_{cr}, this experimental result explains the increase in r_{cr} by the increase of a_{e0} by charge effect.

4.3. DOPC/DPPC QLC

In order to confirm charge effect of lipid head-group, experiments were conducted by mixing DPPC, a neutral lipid molecule, as a control experiment in the same manner as the above experiment. **Figure 9** shows only the QLC below a specific QD size similar to the DOPC QLC experiment results.

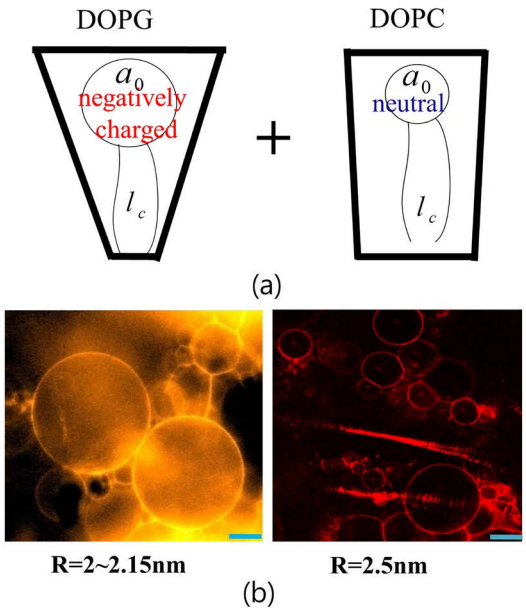

Figure 8. (a) Geometric shapes of DOPG (truncated shape) and DOPC (truncated shape close to cylindrical shape) at a_0; (b) Confocal microscopy image of the QLCs prepared with the same ratio of two lipids DOPC/DOPG (1:1) by using the orange and red-emission QDs (2 - 2.15 (nm) and ~2.5 (nm)). This scale bar is about 10 (μm).

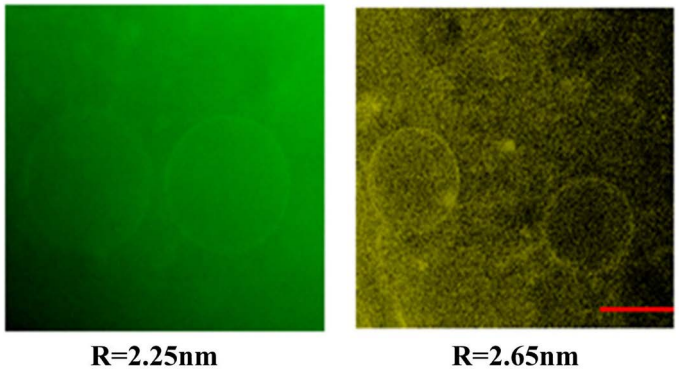

Figure 9. QLC structure using DOPC/DPPC mixed lipid molecules in fluorescence microscopy. This scale bar is about 50 (μm).

In conclusion, it can be expected that the role of charge effect at the head-group is an important factor to form QLC structure above the specific QD size. In this study, unlike previous experimental results, we can observe the orange and red-emission QLC due to highly curvature mono-layer.

5. Conclusion

We proposed a simple model to describe the stability of QDs embedded in lipid bilayer in terms of molecular packing parameter and the conformational change of the lipid chain. The existence of QDs in the lipid bilayer was confirmed using confocal microscopy. QLC formation was found to be dependent on the size of QDs: Egg-QLCs formed with blue, green and yellow-emission QDs (core radius

~1.05 nm, 1.25 nm and 1.65 nm) but not with red-emission QDs (core radius ~2.5 nm). When DOPG lipids, which have a larger head group area, were mixed with DOPC lipids, QLCs were formed with orange-emission QDs as well as with red-emission QDs. The model predicts that 1) QDs below a certain critical size can stably reside in the lipid bilayer, and 2) the specific QD size increases as the head group area of the lipids increases. These predictions agree well with our experimental results in spite of a lack of exact information about the change of effect optimal head area and the conformational changes of the hydrocarbon chain around the QD.

Acknowledgements

This work was supported by a Research Institute for Convergence of Biomedical Science and Technology (30-2018-007), Pusan National University Yang-san Hospital.

References

[1] Park, J., Joo, J., Kwon, S.G., Jang, Y. and Hyeon, T. (2007) Synthesis of Monodisperse Spherical Nanocrystals. *Angewandte Chemie International Edition*, **46**, 4630-4660. https://doi.org/10.1002/anie.200603148

[2] Dubertret, B., Skourides, P., Norris, D.J., Noireaux, V., Brivanlou, A.H. and Libchaber, A. (2002) *In Vivo* Image of Quantum Dots Encapsulation in Phospholipid Micelles. *Science*, **298** 1759-1762. https://doi.org/10.1126/science.1077194

[3] Fan, H., Leve, E.W., Scullin, C., Gabaldon, J., Tallant, D., Bunge, S., Boyle, T., Wilson, M.C. and Brinker, C.J. (2005) Surfactant-Assisted Synthesis of Water-Soluble and Biocompatible Quantum Dot Micelles. *Nano Letters*, **5**, 645-648. https://doi.org/10.1021/nl050017l

[4] Park, S.H., Oh, S.G., Mun, J.Y. and Han, S.S. (2006) Loading of Gold Nanoparticles inside the DPPC Bilayers of Liposome and Their Effects on Membrane Fluidities. *Colloids and Surfaces B*: *Biointerfaces*, **48**, 112-118. https://doi.org/10.1016/j.colsurfb.2006.01.006

[5] Bothun, G.D., Rabideau, A.E. and Stoner, M.A. (2009) Hepatoma Cell Uptake of Cationic Multifluorescent Quantum Dot Liposome*s. Journal of Physical Chemistry Letters B*, **113**, 7725-7728. https://doi.org/10.1021/jp9017458

[6] Chen, Y., Bose, A. and Bothun, G.D. (2010) Controlled Release from Bilayer-Decorated Magnetoloposomes via Electromagnetic Heating. *ACS Nano*, **4**, 3215-3221. https://doi.org/10.1021/nn100274v

[7] Al-Jamal, W.T., Al-Jamal, K.T., Tian, B., Lacerda, L., Bomans, P.H., Frederik. P.M. and Kostarelos, K. (2008) Lipid-Quantum Dot bilayer Vesicles Enhance Tumor Cell Uptake and Retention *in Vitro* and *in Vivo*. *ACS Nano*, **2**, 408-418. https://doi.org/10.1021/nn700176a

[8] Binder, W.H., Sachsenhofer, R., Farnik, D. and Blaas, D. (2007) Guiding the Location of Nanoparticles into Vesicular Structures: A Morphological Study. *Physical Chemistry Chemical Physics*, **9**, 6435-6441. https://doi.org/10.1039/b711470m

[9] Kim, S.J., Wi, H.S., Km, K., Lee, K., Kim, S.M., Yang, H.S. and Pak, H.K. (2006) Encapsulation of CdSe Nanoparticles inside Liposome Suspended in Aqueous Solution. *Journal of Korean Physical Society*, **49**, S684-S687.

[10] Zheng, W.W., Liu, Y., West, A., Schuler, E.E., Yehl, K., Dyer, R.B., Kindt, J.T. and Salaita, K. (2014) Quantum Dots Encapsulated within Phospholipid Membrane: Phase-Dependent Structure, Photostability, and Site-Selective Functionalization. *Journal of the American Chemical Society*, **136**, 1992-1999. https://doi.org/10.1021/ja411339f

[11] Nandi, S., Malishev, R., Bhunia, S.K., Kolusheva, S., Jopp, J. and Jelinek, R. (2016) Lipid-Bilayer Dynamics Probed by a Carbon Dot-Phospholipid Conjugate. *Biophysical Journal*, **110**, 2016-2025. https://doi.org/10.1016/j.bpj.2016.04.005

[12] Gopalakrishnan, G., Danelon, C., Izewska, P., Prummer, M., Bolinger, P.Y., Geissbuhler, I., Demurtas, D., Dubochet, J. and Vogel, H. (2006) Multifunctional Lipid/Quantum Dot Hybrid Nanocontainers for Controlled Targeting of Live Cells. *Angewandte Chemie International Edition*, **45**, 5478-5483.

[13] Wi, H.S., Lee, K. and Pak, H.K. (2008) Interfacial Energy Consideration in the Organization of a Quantum Dot-Lipid Mixed System. *Journal of Physics*: *Condensed Matter*, **20**, Article ID: 494211. https://doi.org/10.1088/0953-8984/20/49/494211

[14] Daniel, M. and Reznickova, J. (2014) Energy of Quantum Dots Encapsulated in Biological Membrane. *Procedia Engineering*, **79**, 137-142. https://doi.org/10.1016/j.proeng.2014.06.322

[15] Wi, H.S., Kim, S.J., Lee, K., Kim, S.M., Yang, H.S. and Pak, H.K. (2012) Incorporation of Quantum Dots into the Lipid Bilayer of Giant Unilamellar Vesicles and Its Stability. *Colloids and Surfaces B*: *Biointerfaces*, **97**, 37-42. https://doi.org/10.1016/j.colsurfb.2012.04.025

[16] Kloepfer, J.A., Cohen, N. and Nadeau, J.L. (2004) FRET between CdSe Quantum Dots in Lipid Vesicle and Water- and Lipid-Soluble Dyes. *The Journal of Physical Chemistry B*, **108**, 17042-17049. https://doi.org/10.1021/jp048094c

[17] Israelachvili, J. (1998) Intermolecular and Surface Forces. Harcourt Brace & Company, New York.

[18] Segota, S. and Tezak, D. (2006) Spontaneous Formation of Vesicles. *Advances in Colloid and Interface Science*, **121**, 51-75. https://doi.org/10.1016/j.cis.2006.01.002

[19] Tanford, C. (1972) Micelle Shape and Size. *The Journal of Physical Chemistry*, **76**, 3020-3024. https://doi.org/10.1021/j100665a018

[20] Holmberg, K., Joensson, B., Kronberg, B. and Lindman, B. (2002) Surfactants and Polymers in Aqueous Solution. John Wiley & Sons, New York.

[21] Li, X.-J. and Schick, M. (2008) Theory of Lipid Polymorphism: Application to Phosphatidylethanolamine and Phosphatidylserine. *Biophysical Journal*, **78**, 34-46. https://doi.org/10.1016/S0006-3495(00)76570-2

[22] Angelova, M.I. and Dimitrov, D.S. (1986) Liposome Electroformation. *Faraday Discussions of the Chemical Society*, **81**, 303-311. https://doi.org/10.1039/dc9868100303

[23] Estes, D.J. and Mayer, M. (2005) Electroformation of Giant Liposomes from Spin-Coated Films of Lipids. *Colloids and Surfaces B*: *Biointerfaces*, **42**, 115-123. https://doi.org/10.1016/j.colsurfb.2005.01.016

[24] Ninham, B.W. and Evans, D.F. (1986) The Rideal Lecture. Vesicles and Molecular Forces. *Faraday Discussions of the Chemical Society*, **81**, 1-17. https://doi.org/10.1039/dc9868100001